DIGITAL TWIN AS A TRANSFORMATIVE APPROACH TO CLASSICAL FORCE MEASUREMENT SYSTEMS

M. J. A. Solis[1], C. Giusca[2], S. Goel[3]

Industrial Technology Development Institute - Department of Science and Technology, Bicutan, Taguig City 1631, Republic of the Philippines, [1] mjasolis@itdi.dost.gov.ph
Cranfield University, Cranfield, Bedfordshire MK43 0AL, United Kingdom, [2] c.giusca@cranfield.ac.uk
London South Bank University, London, SE10AA, United Kingdom, [3] goels@lsbu.ac.uk

Abstract:
Like any other measuring device, load cells are vital in ensuring that products meet quality and safety requirements; therefore, they must always be accurate and reliable. Creep affects measurement results and the useful life of load cells but is not well understood. Digital twins create a virtual representation of an instrument that can be used to understand, monitor, and predict load cell behaviour. This study found that the significant source of creep originates from the strain gauge's carrier matrix and that the Larson-Miller Parameter equation can be used to support the digital twin development of the load cell.

Keywords: creep; load cell; force; digital twin; metrology

1. INTRODUCTION

As safety is paramount in any industry and society, products of any kind must not harm users or the environment. To this end, material/mechanical testing allows the manufacturer to understand, quantify and check whether their product is suitable for a particular application and is safe. This testing process involves the measurement of force/s acting on a product, usually using a load cell. However, creep is a recognised phenomenon that limits the accuracy of the load cells. The slow continuous deformation under constant stress over time may also result in failure or rupture [1]. Therefore, it is necessary that creep is monitored and, if possible, predicted to ensure the accuracy and reliability of the load cell. One such solution is digital twin technology. The digital twin can provide active real-time prediction, monitoring, and recommendation to conduct real-time root cause analysis to avert failures of the load cell [2]. Its purpose is not to mirror but rather to ensure "health," integrity, and reliability through monitoring, prediction, and optimisation of its physical asset using data analytics, artificial intelligence, and machine learning, among others. In this context, the sensors placed on the physical load cell could acquire real-time data through the Internet of Things network. The data can then be used either in simulations or dashboards of information, acting as the load cell's digital twin (Figure 1).
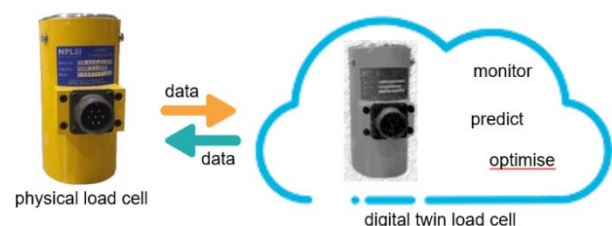

Figure 1: Load cell digital twin diagram

As part of the European Metrology Research Programme EMPIR 18SIB08 Comprehensive traceability for force metrology services (ComTraForce) project, the research presented here was aimed to support the development of a digital twin load cell for creep strain; specifically, the way creep strain influences the reliability of load cells.

1.1. Digital Twin

Product lifecycle management is the most effective way of managing a product from its conceptualisation all the way to its retirement or disposal [3]. Under this context, Grieves, who is the first to coin the term "digital twin," defined it as "a set of virtual information constructs that fully describes a potential or actual physical manufactured product from the micro atomic level to the macro geometrical level", [4]. Grieves describes the technology as having three main components: physical products in Real Space; virtual products in Virtual Space; and connections of data and information that link both products. Being a twin with its own characteristics specific to its physical counterpart, there shall be no twin representing more than one physical asset.

Other researchers added that a digital twin embodies the current state of the physical asset. Its primary role is to monitor the integrity of the asset and determine when and where structural damage is likely to happen. They elaborated that a digital twin provides continuous monitoring and simulation for all system components, including those in

inaccessible or sensitive zones. Setting extreme allowable values to verify compliance by the digital twin enables the identification of instrumentation failures and inconsistencies [5], [6].

1.2. Creep

Creep occurs in all materials in stages; however, they differ on how fast it occurs. The different stages of creep are shown in Figure 2: [7]
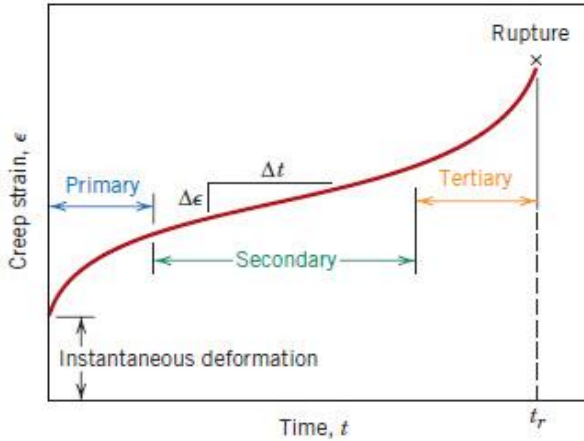

Figure 2: A typical creep curve with its stages

It is acknowledged that creep is mainly evaluated through its creep rate in the secondary stage due to its dominance and long-term occurrence in the creep curve compared to the other stages [8]. Engineers use this information as a point of performance comparison between materials and design for safety assurance by predicting creep behaviour for a particular application. Engineers make use of steady state creep rate $\dot{\varepsilon}_{cr}$ for prediction and extrapolation at different temperatures, and the simplest form of the equation is:

$$\dot{\varepsilon}_{cr} = K \sigma^n e^{\left(\frac{-Q_c}{RT}\right)} \qquad (1)$$

known as the power law equation where K is a constant, σ is the applied stress, n gives the stress dependence of the strain rate, Q_c is the creep activation energy, R is the universal gas constant, and T is the absolute temperature [9]. However, the constants K and n are determined using the existing steady state creep rate obtained from creep data at different stresses and temperatures. This equation is generally used for dislocation and diffusion creep, frequently occurring in metals like stainless steel [10].

Another popular approach is using the Larson-Miller Parameter (LMP) to determine the steady state creep rate. Similar to the power law, it uses existing steady state creep rates obtained from creep data at different stresses and temperatures. The LMP is given as:

$$LMP = T \cdot \left(C - \log(\dot{\varepsilon}_{cr})\right) \qquad (2)$$

where T is the temperature, $\dot{\varepsilon}_{cr}$ is the steady state creep rate and C as the empirical constant which can be obtained from two creep tests conducted at different temperatures but same stress. Li and Dasgupta's work provided the value of C as -3.0 [10]. A master curve is then plotted to show the relationship between the applied stress and LMP. The curve is then used to extrapolate the value of LMP at any given stress to determine the steady state creep rate at any temperature:

$$\dot{\varepsilon}_{cr} = 10^{C - \frac{LMP}{T}} \qquad (3)$$

The dependence of creep in polymers with temperature and time makes the LMP suitable for use with polymers [10].

1.3. Specifications of the Load Cell

This research chose the strain gauge load cell as it is widely used for its accuracy and lower unit cost compared with other types of load cells [11], and it has been the primary focus of the development of the OIML Recommendation 60 [12]. This type uses an analogue resistive element attached to the spring element of a load cell, which changes resistance depending on the deformation of the spring element when a force is applied to the load cell (Figure 3).
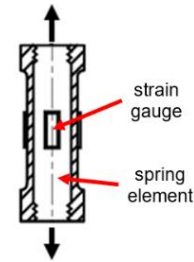

Figure 3: Strain gauge load cell [13]

The basic specifications of the hypothetical 0.5 MN strain gauge load cell used in this research are found in Table 1.

Table 1: Specifications of the hypothetical 0.5 MN load cell

Parameter	Spring Element	Carrier Matrix
Shape	cylinder	rectangular
Material	AISI 316 L(N) stainless steel	polyimide
Young's Modulus	190 GPa	2.5 GPa
Yield Point	-	69 MPa
Height	140 mm	7.5 mm
Diameter	43 mm	-
Width	-	4.6 mm
Thickness	-	30 μm

Spring elements are usually made of stainless steel and aluminium. This choice in the material has to do with the existence of a linear relationship

between the force applied and output with low hysteresis and creep, and a high level of repeatability between force cycles for reliability [13]. The strain gauge is made up of two parts: the carrier matrix and the metal foil pattern as the measuring grid. The carrier matrix is an essential part of the strain gauge since the foil is very brittle and difficult to handle and serves as electrical insulation between the foil and spring element. Nowadays, polyimide is the industry standard and replaces the traditional epoxy since it is stronger and more heat resistant. It can also serve as the adhesive applied at 10 μm thickness between the spring element and carrier matrix [14].

2. DOMINANT SOURCE OF CREEP IN STRAIN GAUGE LOAD CELLS

To investigate the dominant source of creep in strain gauge load cells, the load cell was isolated into two major components: the spring element and the strain gauge. The strain gauge will be represented by its carrier matrix since the measuring grid does not contribute to the creep on the strain gauge, and the carrier matrix makes up most of the strain gauge [13], [15]. For simplicity, the adhesive of the strain gauge was assumed to be part of the carrier matrix and made of the same material [14].

2.1. Determination of Creep Rate in the Spring Element at Room Temperature

The power law given by equation (1) has been used to estimate the creep rate in the spring element of the load cell at room temperature. For this purpose, the experimental data from the work of Reith et al. [16] on the creep behaviour of AISI 316 L(N) stainless steel was used, which allowed the estimation of the creep rate.

The least-square fit method was used in determining the constants of the power law since it assures a more accurate estimation of the constants as it uses all the data points rather than just selected sets [17]. In this case, taking the logarithm of equation (1) transforms it into an algebraic equation:

$$y = a + b\,x + c\,z \qquad (4)$$

where $y = \ln(\varepsilon_{cr})$, $a = \ln(K)$, $b = n$, $c = Q_c$, $x = \ln(\sigma)$ and $z - \frac{1}{RT}$. The constants a, b, and c can be solved by Gaussian elimination using Matlab:

$$aN + b\sum x_i + c\sum z_i = \sum y_i$$
$$a\sum x_i + b\sum x_i^2 + c\sum x_i z_i = \sum x_i y_i \qquad (5)$$
$$a\sum y_i + b\sum x_i y_i + c\sum y_i z_i = \sum y_i^2$$

For convenience, Matlab R2018a software was used. The constants obtained are found in Table 2.

Table 2: Summary of constants for the spring element using the least square fit method

K	7.38×10^3 h^{-1}
n	6.96
Q_c	460 kJ/mol

2.2. Determination of Creep Rate in the Carrier Matrix at Room Temperature

The extrapolation method by LMP was used to determine the creep rate in the carrier matrix given by equation (2). Li and Dasgupta used the experimental creep data of Wu and Pecht [18] to obtain the empirical constant C and creep rates of polyimide. They then used these data to develop an LMP Master Curve for polyimide. Here, the master curve was reconstructed to extract the equation of the resulting trend line (Figure 4).
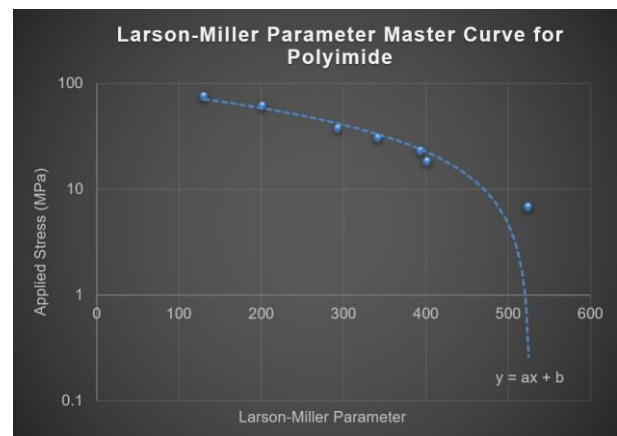

Figure 4: LMP master curve for polyimide

From the equation of the line, the LMP can be determined at a given stress by:

$$x = \frac{y - b}{a} \qquad (6)$$

where x = LMP, y is the applied stress, a = -0.1792, and b = 94.266.

Equivalent Stress Acting on the Carrier Matrix

There is a need to determine the equivalent stress acting on the carrier as a force or stress is exerted at the spring element. Figure 5 is the diagram of the load cell with its spring element, carrier matrix and relationships between different parameters, where F_1 is the force acting on the hypothetical 0.5 MN load cell, L_1 is the length of the spring element, ΔL_1 is the change in length of the spring element due to F_1, A_1 is the area of the spring element where the F_1 is acting on, F_2 is the force acting on the carrier matrix, L_2 is the length of the carrier matrix, ΔL_2 is the change in length of the carrier matrix due to F_2 and A_2 is the area of the carrier matrix where F_2 is acting on.
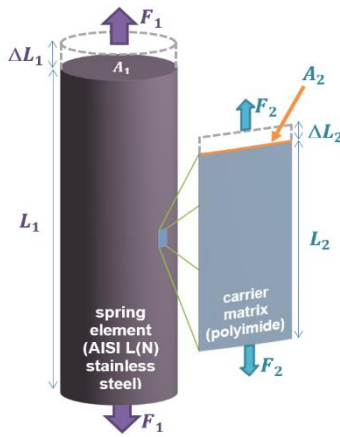
Figure 5: Different parameters acting on load cell

Using the Young's Modulus equation:

$$E = \frac{F\,L_{\mathrm{o}}}{A\,\Delta L} \qquad (7)$$

where F is the force applied, L_{o} is the original length, A is the area where the force is applied, and E is the Young's Modulus of the material, the value of ΔL_1 can be determined by rearranging equation (7) into:

$$\Delta L_1 = \frac{F_1\,L_1}{A_1\,E_{\mathrm{sp}}} \qquad (8)$$

where E_{sp} is the Young's Modulus of AISI 316 L(N) stainless steel. With ΔL_1, equation (9) is used to determine load cell's ΔL_2.

$$\Delta L_2 = \frac{\Delta L_1\,L_2}{L_1} \qquad (9)$$

The force acting on the carrier matrix (F_2) can now be determined by rearranging equation (7) into:

$$F_2 = \frac{E_{\mathrm{cm}}\,A_2\,\Delta L_2}{L_2} \qquad (10)$$

where E_{cm} is the Young's Modulus of polyimide. With this, the stress acting on the carrier matrix can now be computed by dividing the force on the carrier matrix (F_2) by the area of the carrier matrix (A_2). Keying in the stress values to equation (6) provides the corresponding LMP (Table 3).

Table 3: Corresponding LMP values for the force on the hypothetical 0.5 MN load cell

Force on the Load Cell / MN	Equivalent Stress on the Load Cell / MPa	Equivalent Stress on Carrier Matrix / MPa	LMP
0.50	344.30	4.53	501
0.40	275.44	3.62	506
0.30	206.58	2.72	511
0.20	137.72	1.81	516
0.10	68.86	0.91	521

2.3. Results

The equivalent stress on the spring element is needed to extrapolate the creep rate using equation (1). This was determined by dividing the force applied by the area where the force is applied. Finally, extrapolating at the usual working temperature of a load cell (generally 293 K) using equation (1) with the constants in Table 2 yields the creep rates of the spring element at different forces and equivalent stresses. The experimental creep rates from Reith et al. [16] and computed creep rates in the spring element were compared to validate the constants used. It was seen that the differences in values were at 54 % for 923 K, 46 % for 973 K, and 230 % for 1 023 K. These significant differences appear at the higher stress values, whereas in the middle range, the stress values are well predicted. These differences might be due to the lack of data or coverage of the trend to acquire a better estimation of the constants, which is typical during extrapolation or from the errors via the experimental set-up or other factors affecting the outcome of the experimental results. In the same manner, having the LMP makes it possible to extrapolate the creep rates of the carrier matrix at the usual working temperature of a load cell (generally 293 K) using equation (3). The computed creep rates of the spring element and the carrier matrix, presented in Table 4, show that the dominant source of creep originates from the carrier matrix.

Table 4: Calculated creep rates in the spring element and carrier matrix at a given force on the strain gauge load cell

Force on Load Cell / MN	Creep Rate in the Spring Element / h^{-1}	Creep Rate in the Carrier Matrix / h^{-1}
0.50	≈ 0 (3×10^{-58})	1.95×10^{-5}
0.40	≈ 0 (7×10^{-59})	1.88×10^{-5}
0.30	≈ 0 (9×10^{-60})	1.80×10^{-5}
0.20	≈ 0 (5×10^{-61})	1.73×10^{-5}
0.10	≈ 0 (4×10^{-63})	1.67×10^{-5}

3. DETERMINATION OF THE OPERATING PARAMETERS OF LOAD CELLS FOR USE IN DIGITAL TWIN

With the carrier matrix identified as the dominant source of creep in strain gauge load cells at room temperature, the stress-strain curve of polyimide [19] was used to identify the strain due to creep before the strain gauge enters a state where it cannot go back to its original length/shape called plastic deformation.

The strain was determined using equation (11):

$$\varepsilon = \frac{\sigma}{E} \qquad (11)$$

where ε is the strain at yield point σ (69 MPa for polyimide), and E is the Young's Modulus (2.5 GPa for polyimide).

Therefore, the strain at which the carrier matrix undergoes plastic deformation is 2.76 % or 0.0276 (Figure 6). Although the strain of the spring element is likely to be smaller, it should be noted that the deformation, in this case, should be governed by stress and not strain. The spring element will still be in the elastic regime at 69 MPa of stress and will not be much affected; however, that amount of stress is sufficient for enforcing the polyimide by a strain of magnitude 2.76 %. As the spring element is still within the elastic limit, the carrier matrix under a stress of 69 MPa may already be experiencing plastic deformation.
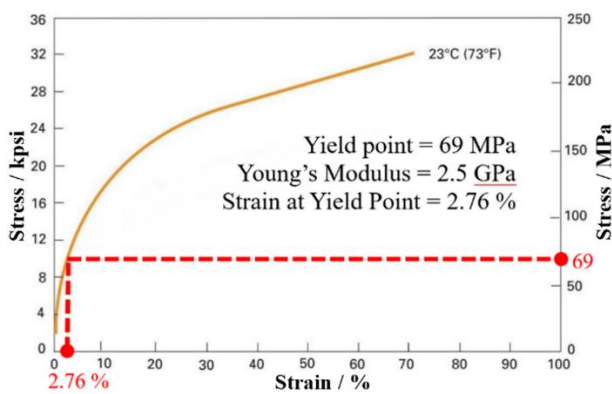

Figure 6: Stress-strain curve of polyimide [19]

3.1. Numerical Model of the Digital Twin Load Cell for Creep Strain

The LMP equation (equation (3)) served as the numerical model after confirming that the strain gauge's carrier matrix is the primary source of creep. Equation (12) shows the expanded version of equation (3) by using equation (6) to replace LMP:

$$\dot{\varepsilon}_{\mathrm{cr}} = 10^{C-\left(\left(\frac{\frac{F}{A}-b}{a}\right)/T\right)} \quad (12)$$

where F is the force applied on the carrier matrix, A is the area where the force is applied, $a = -0.1792$, $b = 94.266$, T is the temperature, and $C = -3.0$ (empirical material constant for polyimide). A and C has been predetermined and inputted in the numerical model, so it only requires two essential inputs to build the digital twin load cell for creep strain: F and T (Figure 7).
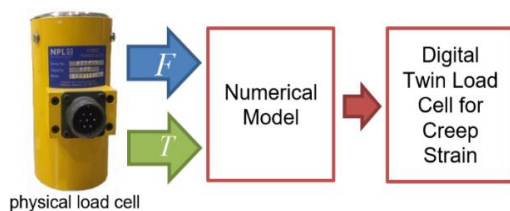

Figure 7: Development of the digital twin load cell for creep strain

The force applied to the carrier matrix can be computed using the method shown in the Equivalent Stress Acting on the Carrier Matrix section, as it receives force measurement data in real-time from the physical load cell. The temperature can be determined by attaching a temperature sensor to the load cell (real-time). This assumes that the spring element's temperature equilibrates with the carrier matrix. With all inputs available, it is possible to determine the creep rates to provide the creep strains. Creep strains were determined by multiplying the creep rate by how long the force is applied. The creep strains were plotted against the force applied to the load cell and the amount of time the force was applied.

3.2. Supporting the Development of the Digital Twin for Load Cell

A digital twin need not be a virtual image of the physical measuring instrument. Instead, the resulting digital twin in this research is represented by a three-dimensional graph in terms of creep strain at the carrier matrix, force applied on the load cell, and amount of time the force is applied.

Figure 8 was developed using Originlab 2019b. The graph represents the digital twin load cell for the monitoring of creep strain and illustrates the operating range of a 0.5 MN capacity load cell with the indication that the creep strain must not exceed 0.0276 when used at room temperature (293 K).
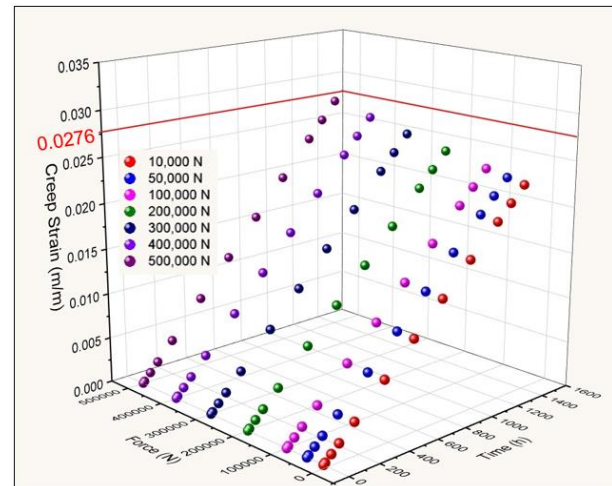

Figure 8: Digital twin load cell for creep strain

Through trial and error, it was revealed that at a maximum load of 0.5 MN, the strain gauge would undergo plastic deformation if the force is applied to the load cell for more than 1 400 hours since the strain at this time is already 0.0276. If the strain gauge reaches this state, the whole load cell has a high risk of becoming defective. Although the usual duration of use of most load cells is not more than two hours, there are applications where load cells are under constant loads for days, such as a calibration system for Coriolis flow meters by

volumetric and gravimetric methods and inventory monitoring of storage silos [13], [20].

The graph also indicates that time influences the creep strain more than the force applied to the load cell. Even at maximum capacity, the creep strain is still lower after one hour compared to an applied force of only 0.01 MN after ten hours. This may look contradictory, but it should be noted that the creep strain at the strain gauge (carrier matrix) is determined by the equivalent stress, which is only 1.31 % of the stress acting on the load cell (Table 3).

4. SUMMARY

The aim of the research was to explore the creep strain digital twin's ability to monitor and optimise the accuracy and reliability of a load cell, and to provide an analytical framework for the development of a digital twin for force measurement systems. The creep strain analytical framework contributes to the development of the overall digital twin of the load cell by providing real-time monitoring, optimisation, and prediction of the creep strain of the whole system to ensure its longevity and reliability. The creep strain values in the digital twin load cell will be updated in real-time as data of applied force and temperatures through sensors are fed into the numerical model from the physical load cell. The digital twin load cell will continuously monitor the creep and issue a warning that measurement should stop, or the strain gauge must be checked for possible onset of damage when the creep strain closely approaches or goes beyond the critical creep strain. With Machine Learning and Big Data technologies embedded within the digital twin, the digital twin load cell can optimise and predict creep behaviour as more data are received.

5. REFERENCES

[1] W. D. Callister, D. G. Rethwisch, Material Science and Engineering. Ninth. John Wiley & Sons (Asia) Pte Ltd, 2015.

[2] NASA, "NASA Technology Roadmaps TA11 - Modeling, Simulation, Information Technology and Processing", 2015.

[3] F. Tao, J. Cheng, Q. Qi, M. Zhang, H. Zhang, F. Sui, "Digital twin-driven product design, manufacturing and service with big data", Int. J. Adv. Manuf. Technol., vol. 94, no. 9–12, pp. 3563–3576, 2018.
DOI: 10.1007/s00170-017-0233-1

[4] M. Grieves, J. Vickers, "Digital twin: Mitigating unpredictable, undesirable emergent behavior in complex systems", in Transdisciplinary Perspectives on Complex Systems: New Findings and Approaches, Springer International Publishing Switzerland, pp. 85–113, 2016.

[5] R. Rosen, S. Boschert, C. Heinrich, "Next Generation Digital Twin", in TMCE 2018, pp. 209–218, 2018.
DOI: 10.17560/atp.v60i10.2371

[6] D. Renzi, D. Maniar, S. McNeill, C. Del Vecchio, "Developing a digital twin for floating production systems integrity management", in OTC Brasil 2017, pp. 1734–1741, 2017.

[7] Total Materia, "Creep and Stress Rupture Properties", 2010. Online [Accessed 20190722].
https://www.totalmateria.com/page.aspx?ID=CheckArticle&site=kts&NM=296

[8] H. Sato, K. Omote, A. Sato, "Extrapolation of Creep Curve and Creep Rate by Strain Acceleration Parameter in Al-Mg Solid Solution Alloys", Mater. Sci. Forum, vol. 794–796, no. 2, pp. 307–312, 2014.
DOI: 10.4028/www.scientific.net/msf.794-796.307

[9] K. Bowman, Mechanical Behavior of Materials. Wiley Inte. Danvers, MA: John Wiley & Sons, 2004.

[10] J. Li, A. Dasgupta, "Failure-Mechanism Models for Creep and Creep Rupture", IEEE Trans. Reliab., vol. 42, no. 3, pp. 339–353, 1993.

[11] R. Kolhapure, V. Shinde, V. Kamble, "Geometrical optimization of strain gauge force transducer using GRA method", Meas. J. Int. Meas. Confed., vol. 101, pp. 111–117, 2017.
DOI: 10.1016/j.measurement.2017.01.030

[12] OIML, Metrological regulation for load cells - Part 1: Metrological and technical requirements, 2021 ed. Paris: OIML, 2021.

[13] A. Hunt et al., "Guide to the Measurement of Force", London, 1998.

[14] A. H. Bracket et al., Strain Gage Users' Handbook. Elsevier Science Publishers, Ltd., 1992.

[15] T. P. Kieffer, "Analysis of Creep Behaviour of Bending Beam Load Cell", Adv. Exp. Mech., vol. 3, pp. 157–160, 2018.

[16] M. Reith et al., "FZKA 7065 Creep of the austenitic steel AISI 316 L (N) – Experiments and Models", Postfach, Karlsruhe, 2004.

[17] A. K. Asraff, R. Aparna, D. Kumaresan, R. Muthukumar, "Comparison of creep properties of four copper alloys and creep based stress analysis of a rocket engine combustion chamber", in Procedia Engineering - 6th International Conference on Creep, Fatigue and Creep-Fatigue Interaction, vol. 55, pp. 45–50, 2013.
DOI: 10.1016/j.proeng.2013.03.217

[18] X. Wu, M. Pecht, "Material Testing for Polyimides", CALCE EPRC, University of Maryland, 1993.

[19] Dupont, "DuPontTM Kapton® Summary of Properties", 2017. Online. [Accessed 20220628]:
https://www.dupont.com/content/dam/dupont/amer/us/en/products/ei-transformation/documents/EI-10142_Kapton-Summary-of-Properties.pdf

[20] T. Kopczynski, D. Ness, "White Paper: Five Factors that can Affect Your Weighing System's Accuracy", San Diego, California, 2011.